MAUSAM, **70**, 3 (July 2019), 501-522

551.509.313

Performance evaluation of WRF model with different cumulus parameterizations in forecasting monsoon depressions

ANANDA KUMAR DAS, P. K. KUNDU*, S. K. ROY BHOWMIK and M. RATHEE

India Meteorological Department, Lodhi Road, New Delhi – 100 003, India

**Mathematics Department, Jadavpur University, Kolkata, India*

(*Received 6 December 2017, Accepted 11 March 2019*)

e mail : akuda.imd@gmail.com

सार – WRF (ARW) मॉडल का उपयोग पाँच भिन्न-भिन्न कपासी प्राचलीकरणों नामत: बेट्स मिलर जांजिक (BMJ), कैन-फ्रिट्च (KF), ग्रील 3 डायमेन्शनल (G3D), Tiedtke (TDK) और नई सरलीकृत अरकावा-शूबर्ट (NSAS) योजनाओं के साथ मिलाकर 2011 के तीन मॉनसून अवदाब परिघटनाओं के लिए तैयार किए गया है। मॉडल के पूर्वानुमान कौशल को प्रेक्षित TRMM.3B42 वर्षा विश्लेषण के साथ सत्यापित किया गया है। पूर्वानुमान की पुष्टि दो दृष्टिकोणों के माध्यम से की जाती है। भारत के क्षेत्र में ग्रिड-प्वाइंट सत्यापन द्वारा ग्रिड-प्वाइंट के लिए मानक श्रेणीबद्ध कौशल स्कोर का उपयोग किया गया है। सन्निहित वर्षा क्षेत्र (सी आर ए) विधि, जो हाल के दिनों में ऋतु उन्मुख सत्यापन तकनीको में से एक है, को आगे के विश्लेषण के लिए भी लागू किया गया है।

मॉडल के वर्षा पूर्वानुमान ने भिन्न-भिन्न कपासी भौतिकी योजनाओं के साथ अलग-अलग प्रदर्शन किया। श्रेणी के अनुसार 5 योजनाओं के तुलनात्मक प्रदर्शन का विश्लेषण संपूर्ण भारत और सात अलग-अलग क्षेत्रों के साथ स्थानिक भिन्नता को दर्शाने के लिए किया गया है। सन्निहित वर्षा क्षेत्र (CRA) विधि का उपयोग करते हुए प्रेक्षण विश्लेषण और मॉडल पूर्वानुमानों में वर्षा के कारणों की तुलना विस्थापन, आयतन और संरचनात्मक त्रुटियों के संदर्भ में की गई है। परिणामस्वरूप प्रेक्षण और मॉडल पूर्वानुमान के बीच वर्षा के तत्वों का प्रतिशत मिलान तुलनात्मक रूप से सभी कपासी भौतिकी के लिए अलग-अलग गणना करके की गई है। यह पाया गया है कि विस्थापन त्रुटि का इसमें प्रमुख योगदान होता है, संबंधित प्रेक्षित प्रवृत्तियों के स्थान से पूर्वानुमान प्रवृत्तियों के रैखिक विस्थापन की भी और स्पष्टता के लिए गणना की गई है। सभी पाँचों योजनाओं के लिए सत्यापन परिणामों की तुलना एक सामान्य धारणा कायम करने के लिए सभी चयनित मौसमी परिघटनाओं के लिए अलग से पूरा किया गया है।

ABSTRACT. Three monsoon depression events of 2011 have been simulated using WRF (ARW) model with five different cumulus parameterizations namely Betts-Miller-Janjic (BMJ), Kain-Fritsch (KF), Grell-3dimensional (G3D), Tiedtke (TDK) and new simplified Arakawa-Schubert (NSAS) schemes. The forecast skills of the model have been verified with observed TRMM-3B42 rainfall analysis. The validation of forecasts is conducted through two approaches. The standard categorical skill scores have used for grid-point by grid-point verification over India domain. The contiguous rain area (CRA) method, one of the object oriented verification techniques in recent times also has been applied for further analysis.

The rainfall forecasts of the model performed variedly with different cumulus physics schemes. The comparative performance of 5 schemes through categorical have been analyzed over whole India and seven separated zones as well to capture spatial variation. Using CRA method the rain objects in the observed analysis and model forecasts have been compared in terms of displacement, volume and structure errors. Consequently, the percentage match of rain objects between observation and model forecast has been computed for all cumulus physics separately for comparison. As the displacement error is found to be major contributor, the linear displacements of forecast objects from the location of respective observed objects have also been computed for further clarity. The comparison of verification results for all 5 schemes has been completed separately for all selected weather events to bring a generalized view.

Key words – Weather Research and Forecast (WRF), Advanced Research WRF (ARW) model, Tropical Rain Measuring Mission (TRMM), Contiguous Rain Area (CRA) method.

1. Introduction

The parameterizations are simplified and idealized representation of complex physical processes in a numerical weather prediction model but it essentially should retain the basic behavior of the process they describe. Therefore, the parameterization schemes by necessity concentrate only on the crucial aspects of the

physical processes limiting the complexity to correctly reproduce the behavior of the process for varieties of environmental conditions.

The outputs from a parametrization scheme are used to step the numerical model state forward in time and generate the time tendencies for most of the model variables temperature, specific humidity, mixing ratios for microphysical particles and the horizontal wind components at each grid point and vertical level. These time tendencies added with other tendencies due to advection and other physical parameterization yield total tendencies for model variables at a certain step of time integration. The update of these tendencies for a parameterization remains constant until the scheme is called again. Therefore, the time between two successive calls and the parameterization scheme play a major role (Bosart, 2003) in determining the time tendencies of model variables and in turn defining the model forecast.

The moist convective process is the most important to the prediction of atmospheric circulation. Large-scale gradient of latent heating produced by deep convection helps to drive vertical circulation and also excites a train of Rossby waves that alter hemispheric flow patterns (Tribbia, 1991). Shallow convection modifies surface radiation budget and has great influence on the modification of boundary layer structure (Randall *et al*., 1985). But the moist convection comprises very small-scale mixtures of updrafts and downdrafts and it is computationally impossible to represent these processes directly on the grids of numerical weather prediction model without cloud resolving resolution (~ 10 to 1000 m). In a convenient approach, various forms of moist convection are divided into two major categories; deep and shallow convection. Deep convection associated with strong updrafts and precipitation, acts to warm and dry the environment. Conversely, non-precipitating shallow convection producing no net warming or drying but vertical dipole effects occur as the convection acts to cool and moisten the upper half of the cloud layer and to warm and dry the lower half of the cloud layer. Moreover, Houze (1997) also showed the convective and stratiform components are often related to each other. Many researcher believe the connective parameterization lose its usefulness since explicit bulk parameterization of microphysics variables of the model grid have been developed. But, the NWP models that are used operationally indeed need grid spacing between 25 to 1000 m to resolve the resolve individual convective elements and the computational requirements to run them still lie a few years in the future.

The cumulus parameterization scheme (CPS) has been developed to suitably estimate the subgrid scale effects of cumulus clouds in a specific NWP model and therefore there are varieties of approaches and assumptions. One of the ways to distinguish them is outlined by Mapes (1977). He separated convective schemes into two general types based upon the vertical extent of the atmospheric forcing that control the convection. Thus CPSs are grouped in two types, e.g., deep-layer control schemes and low-level control schemes. In another way, the schemes are separated by the way convection changes the environment are defined. The static type of scheme determines the final environmental state after convection is done and adjusts the model fields towards the final state. These “convective adjustment schemes” avoid dealing with the details that produce the state and only retain the question that how long it takes the atmosphere to reach the final state. On the other hand, the dynamic scheme considers that the numerous physical processes involved in convection are important and should influence how the scheme functions. These schemes are intended to represent vertical fluxes due to unresolved updrafts and downdrafts and compensating motion outside the clouds (mass flux schemes). The closure assumptions used within a scheme sometimes define where and when convection is activated in the model. The criteria that determine convective development are called “trigger functions and very important to CPS. Some schemes additionally provide cloud & precipitation field tendencies in the column and all of them provide the convective component of surface rainfall (Skamarock *et al*., 2005).

Many studies used WRF model as a regional climate model to study different aspects of monsoon season. Raju *et al*. (2013) tried to study the thermodynamic features of monsoon systems for monsoon 2010 from their seasonal simulation. In another study, Mukhopadhyay *et al*. (2010) compared the error features of WRF model forecasts using different CPSs in their climate simulations. He pointed out the relative performance of those CPSs and advantage of using Betts-Miller-Janjic (BMJ) scheme over other schemes. The following their study, Taraphdar *et al*. (2010) and Kolusu *et al*. (2013) simulated monsoon season high resolution WRF model in regional climate mode with same configuration and studied different phases (active and break) of monsoon. It was understood that the non-linear growth of noise within model forecasts are dependent on different phases of the monsoon. A recent study by Lim *et al*. (2014) simulated summer monsoon rainfall over East Asia with WRF model and investigated the role of resolution with three CPSs (Grell and Freitas, Kain and Fritsch and Betts - Miller - Janjić). The study inferred that the forecast skill of the surface rainfall does not always improve as the spatial resolution increases but the improvement of the probability density function of the rain rate with the smaller grid spacing is robust regardless of the cumulus parameterization scheme.

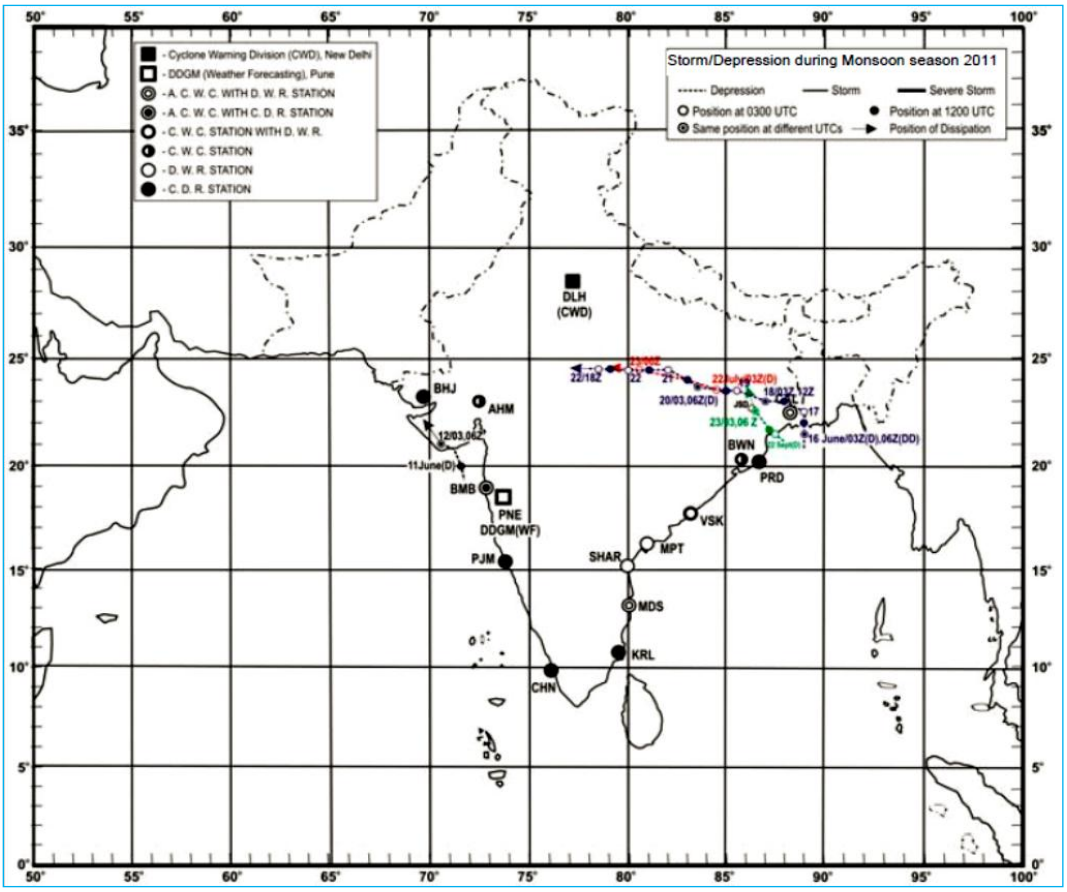

Fig. 1. Storm/depressions during southwest monsoon 2011. Blue track is for Case 1, red track for Case 2 and light green track for Case 3 events respectively

Comparison of CPSs for individual extreme weather events are common over the region and many studies put focus specifically on cyclones (Kanase and Salvekar, 2014; Osuri *et al.*, 2012). A study by Deb *et al.* (2008) compared two CPSs (Kain-Fritsch and Grell-Devenyi) at different rain thresholds in the prediction of heavy rainfall episodes over a specific location in India. The combinations of CPS and cloud microphysics schemes have utility role in predicting monsoon depressions but Wang and Tung (2010) advocated for physics-based high-resolution ensemble forecast. Ardie *et al.* (2012) carried out a comparative evaluation of three different CPSs (Kain-Fritsch, Betts-Miller-Janjic and Grell-Devenyi schemes) in predicting heavy rainfall episodes of monsoon over Malaysia. His study illustrated the case dependency of model performance with the CPSs. The long term WRF simulations over China during monsoon season using same three CPSs by Yu *et al.* (2011) have showed the supremacy of Grell-Devenyi scheme but also depicted the possible cause of forecast deficiencies.

The present study is considering five CPSs and simulating three different rainfall episodes associated with synoptic scale weather systems. But, the comparison of CPSs have been completed the relevant rain areas within the active zone of the system and other influenced rain objects over the region. The evaluation of rainfall forecast of the model has not only done by comparing with point-by-point but also it has been carried out considering individual observed rain object using CRA (contiguous rain area) method.

2. Data and methodology

2.1. *Weather events for case studies*

For the present study of comparative verification of various CPS, three separate weather events during monsoon 2011 have been selected. There had been 10 low pressure areas/well marked low pressure areas which formed during the season. Most of them originated as upper air cyclonic circulations. Five of them formed over the land, four over the Bay of Bengal and one over the Arabian Sea. Out of those low pressure systems, three selected monsoon depression (MD) cases were distinct due to their formation time during the season. The first one in months of June

(a) 0000 UTC on 15th June, 2011

(b) 0000 UTC on 16th June, 2011

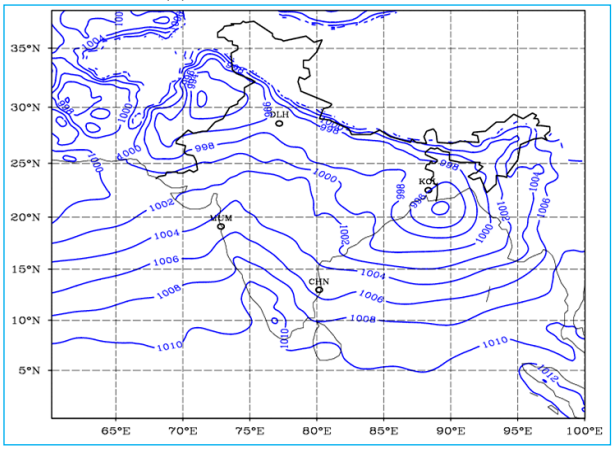

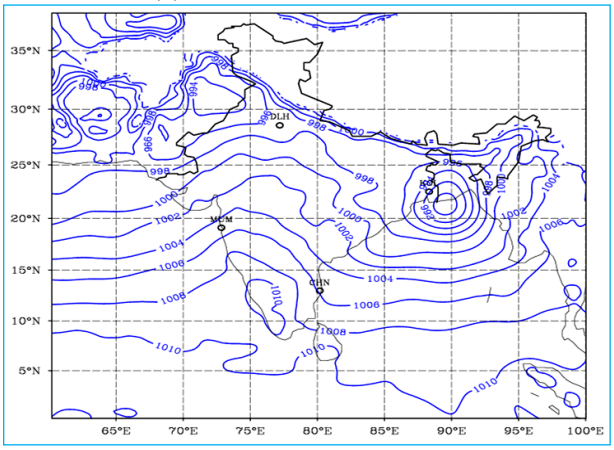

(c) 0000 UTC on 17th June, 2011

(d) 0000 UTC on 18th June, 2011

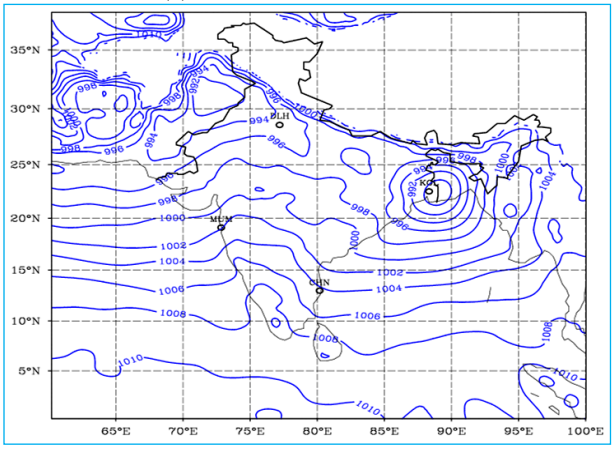

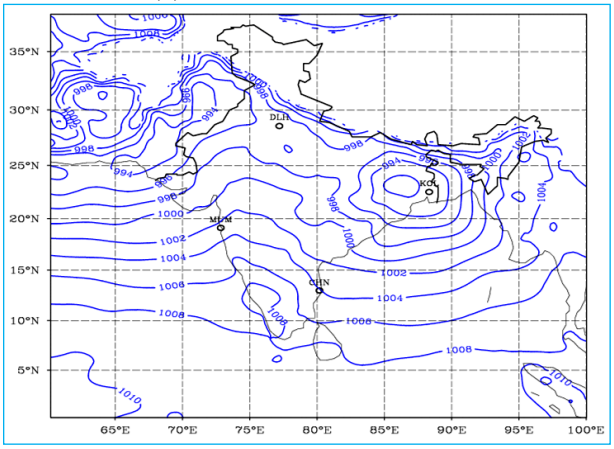

Figs. 2(a-d). The MSLP patterns over Indian region during 15-18 June, 2011 (Case 1)

and happened during the advancement stage of the monsoon. Second one happened in the month of July and mid-season active phase of monsoon. The specific system was a land depression formed over Gangetic West Bengal and adjoining area but produced significant rain over the region. The last one occurred at the time of withdrawal of monsoon and remained confined over a region adjacent to head Bay and neighborhood.

The estimated tracks of all three systems by India Meteorological Department (IMD) are shown in Fig. 1. The four days during each event have been considered for the model simulation and respective verification of day 1 and day 2 completely spanned over the lifecycle (~ 5 days) of the synoptic events.

Case 1 : *Monsoon Depression (16-23 June, 2011)*

A well-marked low pressure area formed over the northwest Bay of Bengal and neighborhood on 15th June, 2011. It concentrated into a Depression and lay centered at 0300 UTC of 16 over the northwest Bay of Bengal, near 21.5° N/89.0° E and further intensified into a Deep Depression at 0600 UTC of same day. It further moved north northwestwards and crossed West Bengal-Bangladesh coasts, between 1100 and 1200 UTC of 16. Moving slightly northwards, it lay centered near 22.5° N/ 89.0° E, at 0300 UTC of 17 and subsequently moving westwards lay over Gangetic West Bengal, near 23.0° N/ 88.0° E, at 1200 UTC of the day. Further moving westwards, it centered near 23.0° N/87.0° E, at 0300 UTC of 18. It remained practically stationary over Gangetic West Bengal and adjacent Jharkhand region till evening. Thereafter, it further moved northwards and lay centered near 23.5° N/ 85.5° E at 0300 UTC of 19 and moving slightly westwards near 23.5° N / 85.0° E at 1200 UTC of the day. It continued to move west northwestwards over the region in the morning of 20 and further weakened into a Depression 0600 UTC. Then, the system propagated in a northwestward direction over southeast Uttar Pradesh and neighborhood.

(a) 0000 UTC on 20th July, 2011

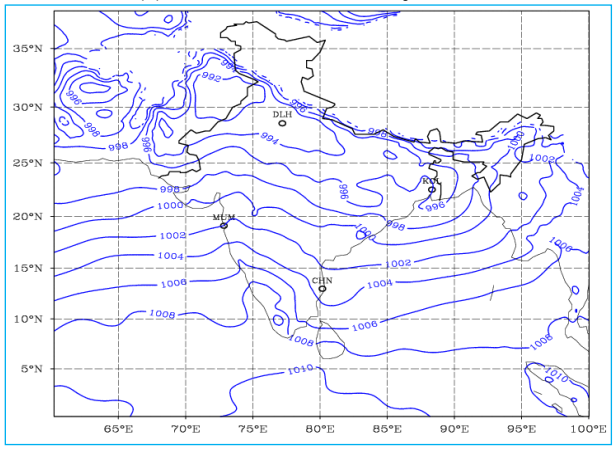

(b) 0000 UTC on 21st July, 2011

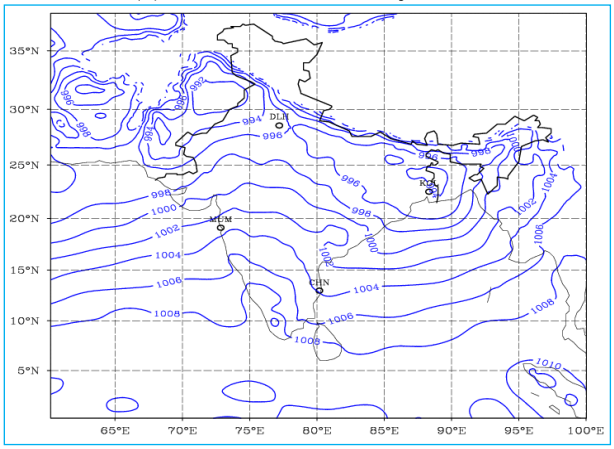

(c) 0000 UTC on 22nd July, 2011

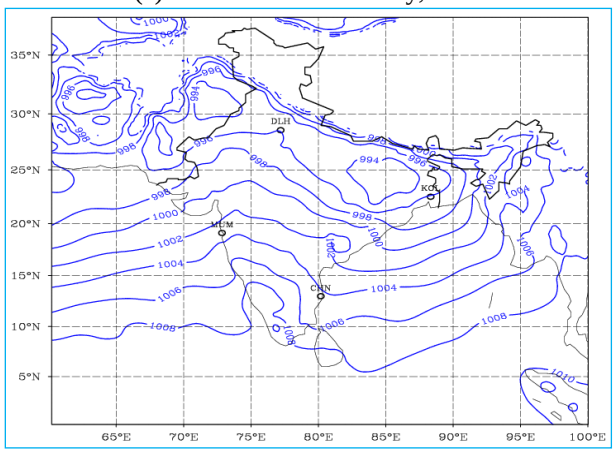

(d) 0000 UTC on 23rd July, 2011

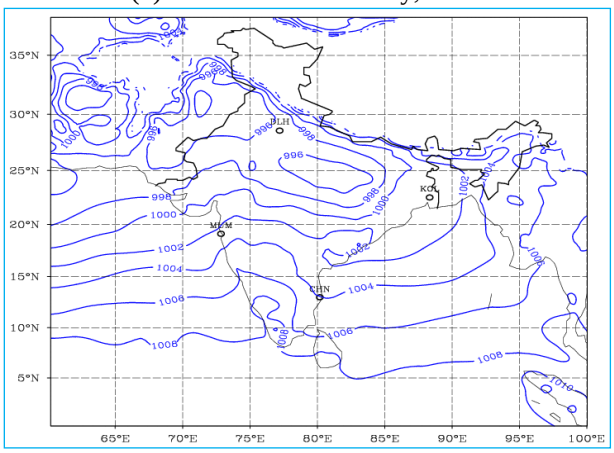

Figs. 3(a-d). The MSLP pattern over Indian region during 20-23 July, 2011 (Case 2)

Subsequently moving west northwestwards, in the morning of 21 the system reached over east Madhya Pradesh and adjoining south Uttar Pradesh. It continually moved westwards over east Madhya Pradesh till 0300 UTC of 22 and positioned over the central parts of Madhya Pradesh and adjoining south Uttar Pradesh, at 1200 UTC. It moved further northwestwards and weakened into well marked low pressure area over west Madhya Pradesh and neighborhood in the early morning of 23. The mean sea level pressure (MSLP) patterns in the WRFDA analyses at 0000 UTC during 16 to 18 June, 2011 of the event are shown in Figs. 2(a-d).

Case 2 : *Land Depression over Jharkhand (22-23 July, 2011)*

Under the influence of the low pressure area formed over Gangetic West Bengal and neighborhood, a Depression formed over northwest Jharkhand and neighborhood, at 0300 UTC of 22nd July, 2011. Moving in a west northwesterly direction, it lay over southeast Uttar Pradesh and neighborhood, at 1200 UTC of same day. Thereafter, it moved westwards and lay centered over east Madhya Pradesh, at 0000 UTC of next day. Continuing the westward movement, it weakened into a well-marked low pressure area and lay over north Madhya Pradesh and neighborhood on 23 morning and became less marked on 24. Figs. 3(a-d) show the MSLP patterns at 0000 UTC for four consecutive days of the event 20-23 July, 2011.

Case 3 : *Monsoon Depression (22-23 September, 2011)*

The third selected depression during monsoon 2011 formed towards the end of the season (22-23, September). In association with an active monsoon trough, a low pressure area formed over the North Bay of Bengal on 21st September, 2011. The vertical wind shear of horizontal wind between 850 and 200 hPa was low to moderate (10-20 knots). There was increase in lower level

(a) 0000 UTC on 20th September, 2011

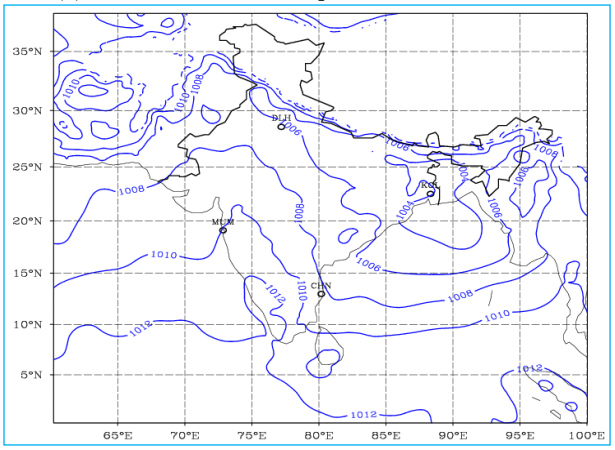

(b) 0000 UTC on 21st September, 2011

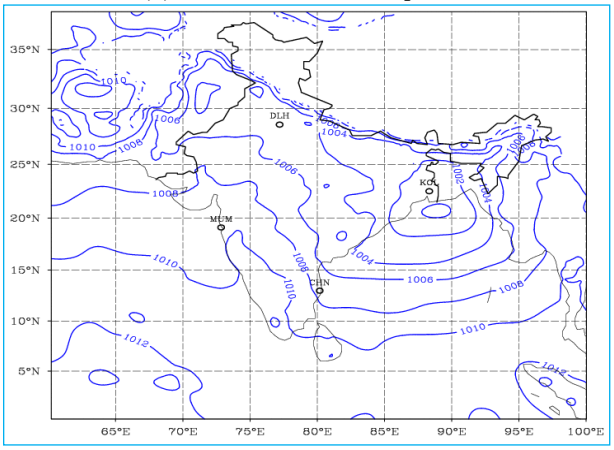

(c) 0000 UTC on 22nd September, 2011

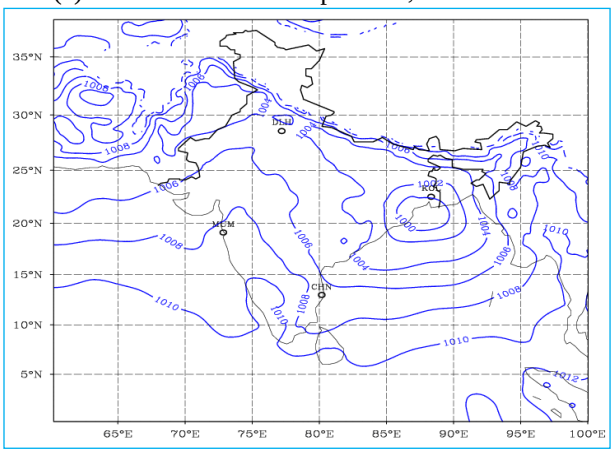

(d) 0000 UTC on 23rd September, 2011

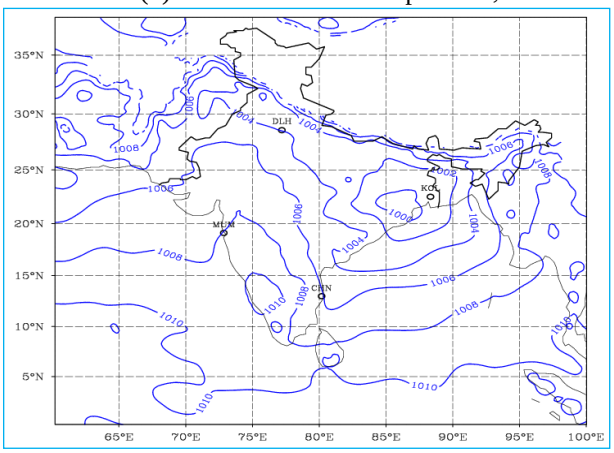

Figs. 4(a-d). The MSLP pattern over Indian region during 20-23 September, 2011 (Case 3)

relative vorticity and upper level divergence also over the region. Under these favorable synoptic and environmental conditions, the low pressure area concentrated into a depression at 0300 UTC of 22nd September, 2011 over the northwest Bay of Bengal near 21.5° N / 87.5° E. It moved slightly westwards and lay centered near 21.5° N / 87° E at 1200 UTC and then moving west northwestwards, crossed north Orissa coast, between 1700 and 1800 UTC of 22. Subsequently moving northwestwards, it lay over Jharkhand and neighborhood, at 0300 UTC of 23. It remained practically stationary over the region and weakened into a well-marked low pressure area by 0900 UTC. The patterns of MSLP during this event are shown in Figs. 4(a-d).

2.2. *Model and data*

The WRF model is considered with its non-hydrostatic and full physics configuration (described in Table 1). The initial condition is provided from mesoscale assimilation system WRFDA and boundary condition has been derived from GFS forecasts and updated accordingly as per mesoscale analysis. The different experimental setups have been customized with various cumulus parameterization schemes. The schemes have been selected on the basis of their functioning inside the model as each of them has distinct formulation feature. In the present study, five (5) cumulus parameterization schemes have been employed and evaluated sensibly using the standard and object oriented verification techniques. In the next sub-section, we are briefly describing necessary intricacies of the schemes to distinguish them separately.

The model has been integrated for two days using initial conditions at 0000 UTC of four consecutive days during each weather event. Five set of forecasts for a day has been generated separately with five CPSs keeping all other model configuration intact. The numerical experiments with all CPSs have been repeated for all three cases. The forecast parameters from model forecasts have

been computed and processed from the native model output using NCAR Command Language data analysis and visualization tool (NCL, 2013).

2.3. *Numerical experiments with cumulus physics*

The WRF model framework is capable of incorporating different CPS with other physics schemes. The numerical experiments are designed and named as per used CPSs. Five cumulus schemes chosen to be tested in the present study are as follows:

(*i*) *Betts-Miller-Janjic (BMJ)*

(Janjic, 1994) : The deep convection profiles and the relaxation time are variable and depend on the cloud efficiency, a dimensionless parameter that characterizes the convective regime. The shallow convection moisture profile is derived from the requirement that the entropy change is small and nonnegative (Janjic, 1994). The scheme adjusts the sounding towards a pre-determined, post convective profile derived from climatology. This post convective profile which can vary with season and location is defined by points at the cloud base, cloud top and freezing level. The original sounding adjusted to the post convective profile produce a net change in precipitable water as well as in net heating and cooling. Convective initiation takes place when profiles are moist through a deep layer of the atmosphere and convective available potential energy (CAPE) and convective cloud depth thresholds are exceeded.

(*ii*) *Kain-Fritsch Scheme (KF)*

(Kain, 2004) : The scheme utilizes a simple cloud model with moist updrafts and downdrafts, including the effects of detrainment, entrainment and relatively simple microphysics (Skamarock *et al*., 2009). Shallow convection is allowed for any updraft that does not reach minimum cloud depth for precipitating clouds and this minimum depth varies as a function of cloud-base temperature. For downdrafts, the source layer is the entire 150-200 hPa deep layer just above cloud base, mass flux is specified as a fraction of updraft mass flux at cloud base, fraction is a function of source layer relative humidity and detrainment is specified to occur in updraft source layer and below. The entrainment rate varies as a function of low-level convergence. The changes to the sounding temperature are a result of cloud detrainment, subsidence and evaporation driven downdrafts into the convective source level. The closure is designed to rearrange mass in a column so that CAPE is consumed (or eliminated). The scheme evaluated CIN by the amount of negative area and must be small enough for the parcel to penetrate. Also only positive buoyancy is necessary to

TABLE 1

WRF model configuration (version 3.4)

Domain	
Horizontal grid distance	27 km
Integration time step	120 second
Number of grid points	X-direction 335 grid points (60° E, 120° E) Y-direction 315 grid points (23° S, 46° N)
Vertical levels in First guess analysis	27
Vertical co-ordinate	Terrain-following eta co-ordinate (38 levels)
Model P-top	50 hPa
Physics	
Microphysics	WSM 5 class mircrophysics
Radiation Scheme(Long-wave)	RRTM scheme
Radiation Scheme(short-wave)	Goddard short-wave scheme
Minutes between radiation physics calls	10
Surface layer physics	Monin-Obukhov (Janic) scheme
Land-surface parameterization	Unified Noah land-surface model
PBL parameterization	Mellor-Yamada-Janjic TKE scheme
Time between two successive PBL physics calls	0 minutes
Cumulus parameterization schemes	5 different schemes have been selected
Time between two successive cumulus physics calls	5 minutes
Dynamics	
Dynamic option	Eulerian mass (ARW)
Time Integration	3rd order Runge-Kutta
Vertical velocity damping flag	1 - damping is imposed
Turbulent and mixing option	1 - evaluate 2nd order diffusion terms
Eddy coefficient option	1 - constant values eddy diffusion co-efficient
Damping coefficient	0.02
Number of sound steps per time-step	4
Spatial differencing scheme	6th order centered differencing
Dynamics	Non - hydrostatic
Others	
Bottom Boundary condition	Physical or free-slip
Map Projection	Mercator
Horizontal grid distribution	Arakawa C-grid
Main prognostic variables	u, v, w, p′, θ′, Φ′
Number of domain	Single Domain
Central point of the domain	Central Lat.: 14.0° N and Central Long.: 80.0° E
Initial conditions	3-dimensional real-data (FNL: 0.5° × 0.5°)
Lateral Boundary condition	Specified options for real-data
Top boundary condition	Gravity wave absorbing (diffusion or Rayleigh damping)

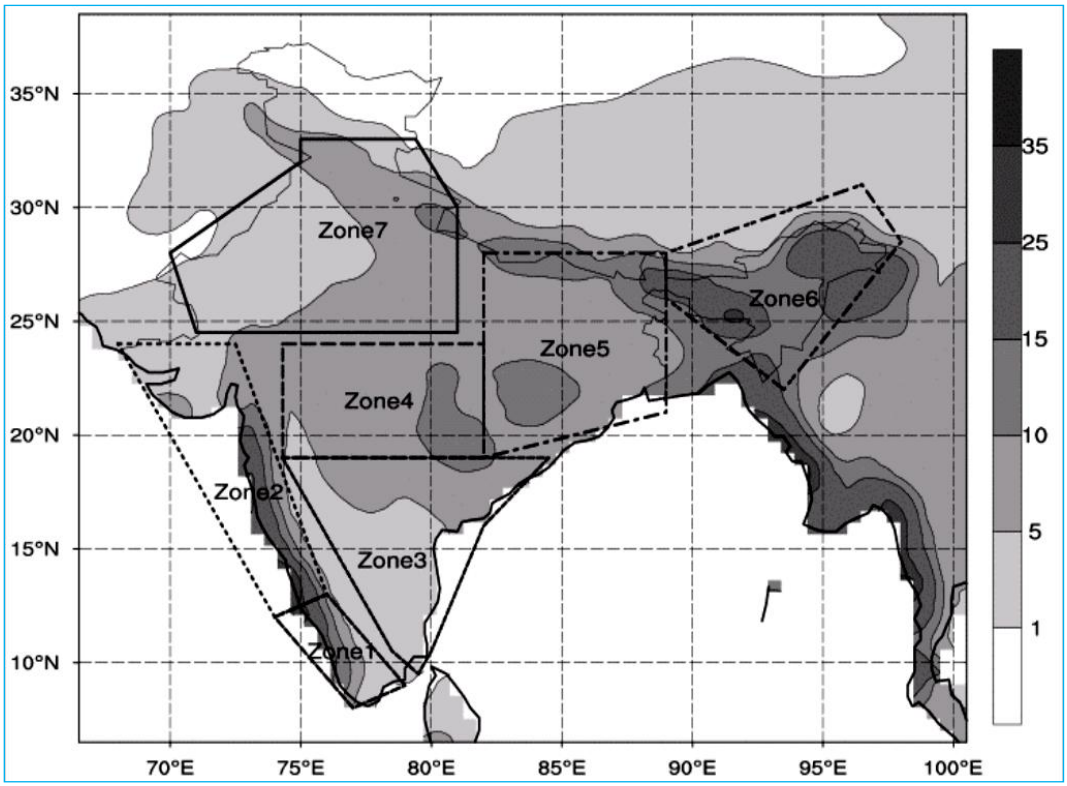

Fig. 5. Locations of seven geographical regions for rainfall verification along with GPCC climate normal rainfall (mm/day)

initiate convection and the intensity of convection in the model using KF is a function of instantaneous CAPE as opposed to CAPE changing with time.

(*iii*) *Grell-Devenyi 3D ensemble (G3D)*

(Grell, 1993; Grell and Devenyi, 2002) : This is an ensemble cumulus schemes in which effectively multiple cumulus schemes and variants are run within each grid box & then the results are averaged to give the feedback to the model state. The schemes are mass-flux type schemes but with differing updraft and downdraft entrainment and detrainment parameters and precipitation efficiencies. The differences between all ensemble members are in static control combined with differences in dynamic control, which is the method of determining cloud mass flux. The dynamic control closures are either based on CAPE, cloud work function or moisture convergence.

(*iv*) *Tiedtke Scheme (TDK)*

(Tiedke, 1989; Zhang *et al*., 2011) : The TDK is a convective parameterization scheme used in the ECMWF (European Center for Medium-Range Weather Forecasting). Convective clouds form as a result of the detrainment of cloud air from convective updrafts into environmental air. The clouds are dissipated by heating (adiabatic and diabatic), formation of precipitation and turbulent mixing between cloud air and drier environmental air at cloud edges. There is no difference between the way convective clouds and other cloud forms within precipitation processes. A new trigger is added which is based on a diluted air parcel testing, while the old trigger is based on the moisture convergence. New organized entrainment and turbulent entrainment/ detrainment rate for deep convection based on ECMWF method is added (Zhang *et al*., 2011).

(*v*) *New Simplified Arakawa-Schubert Scheme (NSAS)*

(Han and Pan, 2011) : This scheme based on simplified Arakawa-Schubert scheme (SAS) previously used operationally in the global forecasting system of NCEP, but many aspects in the previous SAS scheme such as cloud-base mass flux, entrainment and detrainment specifications have been modified to accommodate the shallow convection. The random cloud-top selection in the SAS scheme is replaced by an entrainment rate approach with the rate being dependent on environmental moisture. A modification of the triggering function has also been developed. The new shallow convection scheme employs a mass flux parameterization, which is more physically appropriate than the old (turbulent diffusion) scheme and the cloud-

base mass flux is given as a function of the convective boundary layer velocity scale. Therefore, the long standing problem with systematic underestimation of stratocumulus clouds has been targeted by modifying the shallow convection scheme. The SAS deep convection scheme has been revised in order to suppress the unrealistic grid-point storms, which are believed to result from the convective parameterization not fully eliminating the instability and consequently causing explicit convective ascent to occur on the grid scale.

2.4. *Comparative verification strategy*

The verification of models forecasts from all different numerical experiments mentioned above is necessary part of the study. The three verification methodologies followed to complete the comparative analysis on the impact of different cumulus parameterizations in WRF model. The validation of forecasts from all physics experiments have been completed against observation and improved mesoscale analysis. A few diagnostics on forecast parameters also been computed to support the performance evaluation. The observed rainfall analysis (3 hourly 3B42) from Tropical Rainfall Measuring Mission (TRMM) with 0.25° × 0.25° resolution has been considered as truth for the rainfall verification. The rainfall forecasts from the model has been interpolated and remapped to the same grid structure of verification analysis from its native 27 km resolution. The accumulation period (0300 UTC to 0300 UTC) has also been matched between TRMM analysis and model forecast.

In the first approach, the standard validation study on rainfall forecasts has been carried out with an investigation of skill scores and the MET (Model Evaluation Tools, 2011) has been utilized for this purpose. The scores have been computed for whole India as well as 7 geographical zones (shown in Fig. 5). The descriptions of the zones are given in Table 2.

Secondly, we have employed CRA verification to know the contributions from different partitions (e.g., displacement, pattern and volume) of error generated in different physics experiments. The CRA verification study in this paper is based on object-oriented CRA method described by Ebert and Gallus (2009). Overall benefit of CRA verification technique has been established during whole monsoon season over the Indian region has been established in the previous studies by Das *et al*. (2014, 2015) using the daily forecasts by WRF model. The method has been employed with gridded rainfall analysis (IMD and TRMM3B42).

Independently for each day during each case, all CRAs have been defined and then selected following the CRA algorithm for four selected thresholds (*i.e.*, 21.5, 35.5, 50.0 and 64.5 mm daily rainfall). The CRAs are stenciled separately for four different thresholds in a day and every individual CRA has been considered to make a match between observed and forecast fields. The forecast error for each CRA has been computed with three partitions, *i.e.*, displacement, pattern and volume errors. The mean value has been computed considering all CRAs for a certain threshold happened during the case irrespective of their locations and the days of occurrence. The CRA method has been employed separately for day 1 and day 2 forecasts but only results of day 1 has been considered for discussion. The matching criteria have been set to find the matches for the observed CRAs for a certain threshold. The specific observed object has been searched over respective forecasts and search has been continued as long as the maximum value of spatial correlation coefficient ≥ 0.4 (which statistically significant with level of significance 0.05 for a template having minimum of 20 points). As soon as the match is found for an observed object, the shift of respective forecast object has been computed from the initial and final positions of center of mass. When the matching criteria have not been satisfied for a certain observed CRA, the object is considered to be missed in the forecast. During the entire duration, the match or miss statistics of all observed CRAs have been computed for different rainfall thresholds. The number matches found in the forecasts for observed CRAs has also been compared.

TABLE 2

Seven geographical regions considered for rainfall verification

Zone name	Geographical region of India	Abbreviated name
Zone 1	Kerala	KRL
Zone 2	West Coast	WC
Zone 3	Southern Peninsula	SP
Zone 4	Central India	CTR
Zone 5	East India	EI
Zone 6	North-East India	NE
Zone 7	North-West India	NW

3. Results and discussion

The results of all three different weather events will be discussed in this section but the first weather event (Case 1) will be given a bit priority for the investigation of a few features related to the study. Altogether, the focus will be on the specific similarities or distinct contrasts amongst numerical experiments with different CPSs. Within the discussion, several segments will lay the linkages between the aspects of results. The main moto of

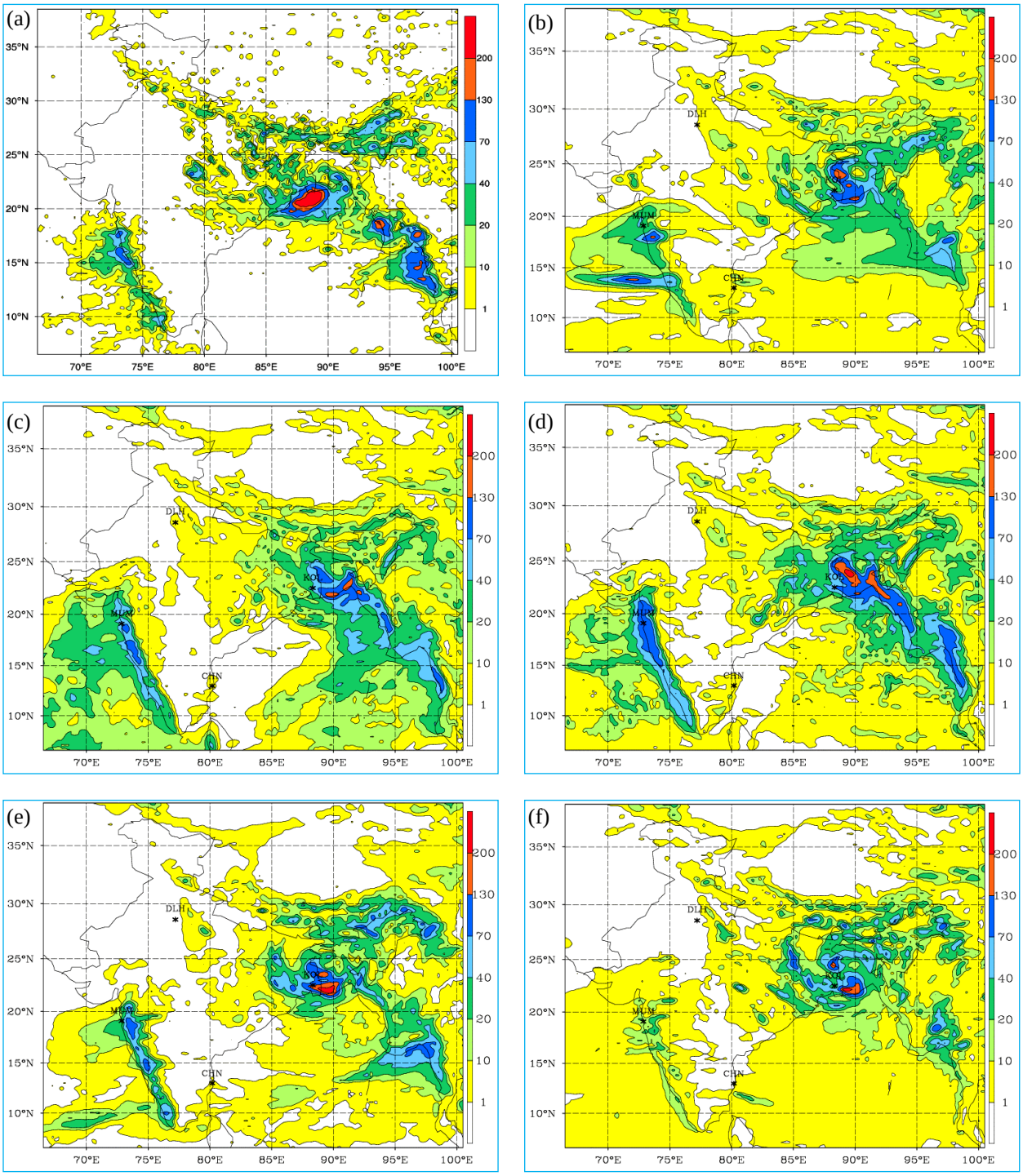

Figs. 6(a-f). Observed and day 1 forecasts of rainfall valid at 0300 UTC of 17th June, 2011. (a) for observed TRMM rain and rainfall forecasts are for (b) BMJ, (c) G3D, (d) KF), (e) TDK and (f) NSAS respectively

the study is the comparison between five CPSs in predicting rainfall over the region and discussion of other related meteorological parameters have been omitted in the present investigation. In the course of deliberation, rather putting weightage to the characteristics of all three weather events, prominent comparative features in the model forecasts by different physics experiments have been given emphasis. Three kinds of verification approach mentioned in the last section have been followed and the sequencing of sub-sections is deliberated accordingly.

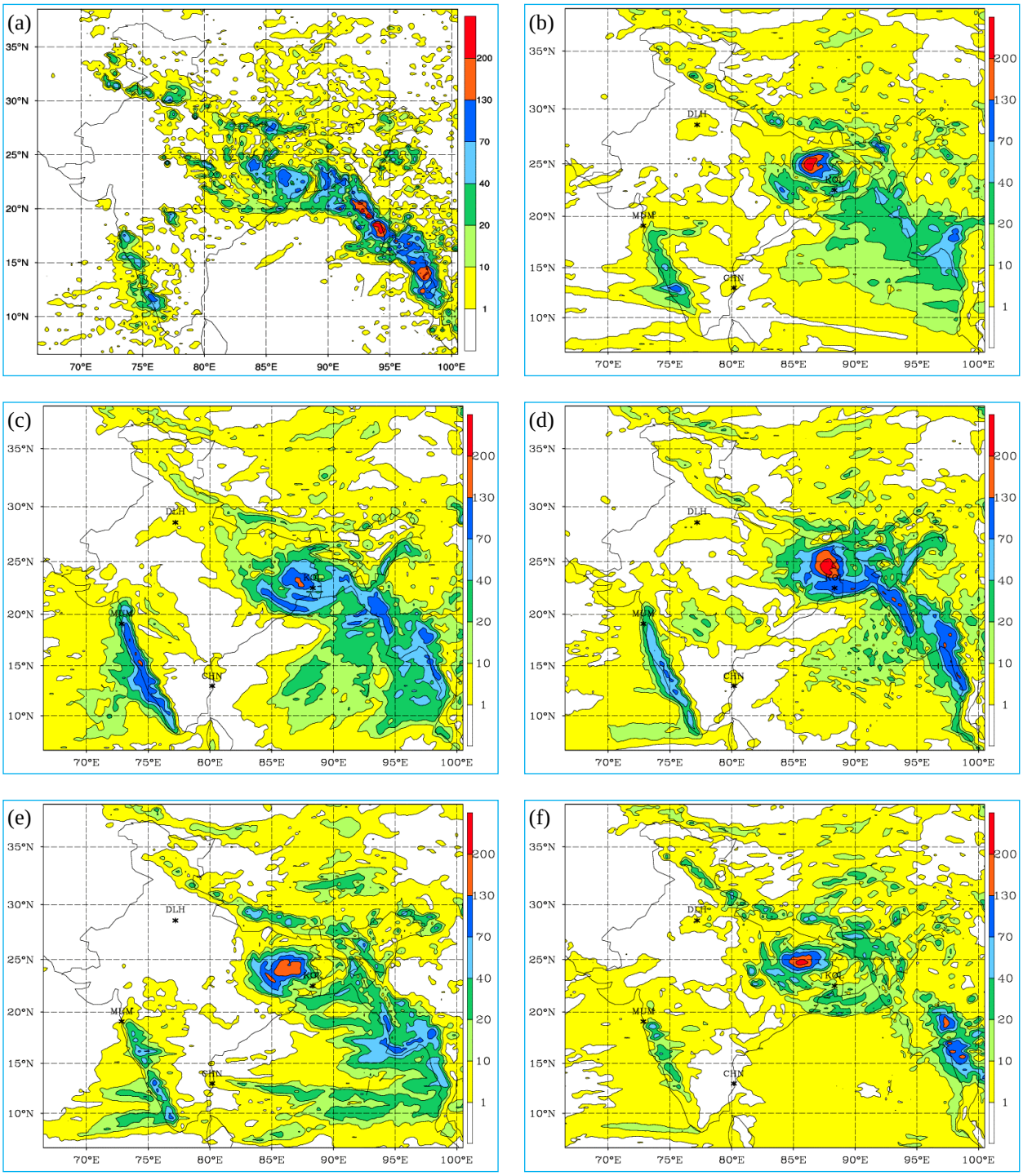

Figs. 7(a-f). Observed and day 2 forecasts of rainfall valid at 0300 UTC of 18th June, 2011. (a) for observed TRMM rain and rainfall forecasts are for (b) BMJ, (c) G3D, (d) KF), (e) TDK and (f) NSAS respectively

3.1. *Verification of rainfall forecasts using standard skill scores*

Before the discussion of different skill scores, the spatial distributions of daily observed rainfall (TRMM accumulated from 0300 UTC of a day to next day 0300 UTC) along with respective forecasts (day 1 and day 2) over the Indian region from all physics experiments have to be looked upon for an eyeball assessment. For an exploratory analysis, only spatial

rainfall patterns of first weather events (Case 1) has been considered.

Figs. 6(a-f) show the day 1 rainfall forecasts from all 5 physics experiments along with observed TRMM rain over the Indian region valid at 0300 UTC of 17 June, 2011. The prominent rainfall belts (enclosed within dotted ellipses) along west coast of India and Arakan coast due to orographic effect are visible in all panels but with varied intensity and spatial extent. The prominent observed rainfall distribution (the area outlined by dotted thick black line) near head bay region is associated with the MD. The other noticeable rainfall belt (outlined by dotted thick black line) is over Western Ghats along west coast of India. In the figure, it is evident that all physics experiments have produced significant rainfall due to weather system. But, the location, intensity and pattern of the rain objects in their forecasts have lots of variation. In the Figs. 7(a-f) day 2 forecasts of the model are valid at 0300 UTC of 18th June, 2011. The all panels are similar to Figs. 6(a-f) but represent the rainfall for the specific day. In a similar fashion, the day 2 forecasts of all experiments also have lots of variation amongst them and it is very difficult to compare and reach to a clear-cut conclusion. Only an idea about the representation of different rainfall areas can be gathered from eye-ball verification. Looking at the spatial patterns of rainfall associated with the depression, it can be noticed that there are mismatched between the observed and forecast rain belts in terms of their location and phase of the weather system. The model portrayed weather situation in different manners with various CPSs. It is easily detected that the observed maximum rainfall during day 1 is under predicted by all forecasts but an obvious overestimation is seen during day 2. The forecasts for both G3D and KF have gross feature of rainfall spreading over whole region near to depression but KF has more pronounced maxima. The nearly similar displacements of rainfall belts in the forecasts for all CPSs except KF are visible in Figs. 6(a-f). But the forecast rain areas during day 2 for different CPSs have wide variation amongst them. Now, it is apparently staggering tasks for the standard skill scores to make fair comparison amongst CPSs.

Three different skill scores have been selected for the verification, e.g., threat score or critical success index, equitable threat score or Gilbert skill score and bias score. The Figs. 8(a-o) illustrate the categorical skill scores of all forecasts for different rain thresholds of 0.1 (rain/no-rain), 2.5, 7.6, 35.5 and 64.5 mm. The various rows of the figure are representative of different geographical regions, *i.e.*, whole India, CI, EI, WC and NW (descriptions of the regions are given in Fig. 5 and Table 2). From the values of TS and ETS it is clear that for a rainy day forecast BMJ and TDK have better performance compared to others. For rain thresholds of 2.5 and 7.5 mm, all experiments show comparable skill of the model considering whole India region. Over various zones, the experiments display variation and CPSs do not follow any specific relation. The all India average has lower values of skill scores compared to individual zones within. The TS score is not able to show significant dissimilarities between experiments but tells that over CI zone the model perform poorly compared with other zones. The BIAS score signifies the overestimation of rainfall over all regions for all lower rain thresholds. All experiments have similarity in this aspect. The model performance degrades from day 1 to day 2 forecasts as the skill scores values have lower values in Figs. 9(a-o) (skill scores of day 2 forecasts) but BIAS score shows the reduction in overestimation.

The poorest skill over CI and NW zones may be due to rare occurrences of rainfall events very high values both in observation and forecasts as well. It is also seen in Figs. 8(a-o)&9(a-o), that the heavy rainfall is confined over EI and WC zones mostly during this event. The EI has comparatively more points with higher rain and the ETS scores are bound to skew away from 0.1 mm category. The KF has edge over others at higher thresholds and over the region (WC, EI) with higher observed rainfall during the event. This is also true for day 2 forecasts of the model with KF. The TDK and NSAS have prominent variation from day 1 to day 2 more specifically over CI and NW. The G3D and KF schemes have significant variations between zones and but have similarity in forecast hours.

The spatial plots of observed rainfall at 0300 UTC on 22 July of 2011 is shown in Fig. 10(a) whereas other panels in Figs. 10(b-f) show the forecasts from 5 physics experiments. Looking at the patterns of prominent rainfall objects, it is clear that the model with every CPS poorly captured their location and features as well. But, the forecast of the model fairly captured the prominent rainfall zones in a better way during Case 1. But, it is not reflected well through the evaluation with skill score values. The skill scores are computed over thresholds at each grid points and do not take into account the rainfall situation of the adjacent points but count the hits and misses. The skill scores for day 1 forecasts of Case 2 are plotted in Figs. 11(a-o). The scores are not skewed over threshold range as the rainfall distribution during this event (mid-season) is covers whole Indian region. But, the experiments show similar comparative features with slight variation in their values. The overestimation is again noticed up to moderate thresholds and KF and G3D also similar enhanced overestimation over WC zone during Case 2. As the system formed over EI and moved further westward, the rainfall zone usually resided west of EI zone during the event. Therefore, the rainfall amount is smaller over EI as compared to Case 1. The same is

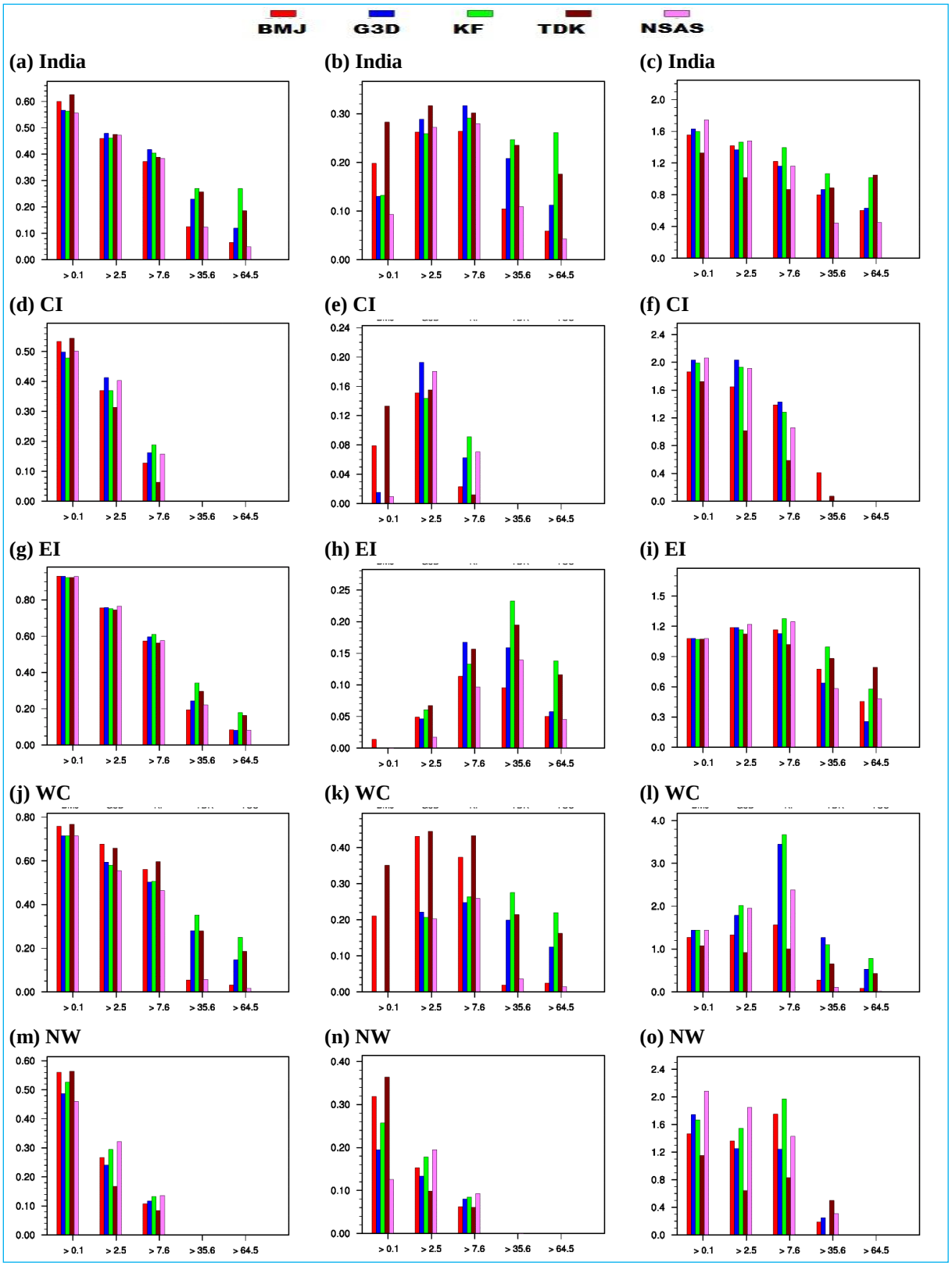

Figs. 8(a-o). Three categorical skill scores of day 1 forecasts for all physics experiments during case studies of 16-18 June, 2011. Left most panels for CSI, middle panels for GSS and right panels for FBIAS scores. (a), (b) and (c) for all India, (d), (e) and (f) for CI, (g), (h) and (i) for EI, (j), (k) and (l) for WC and (m), (n) and (o) are for NW zones respectively

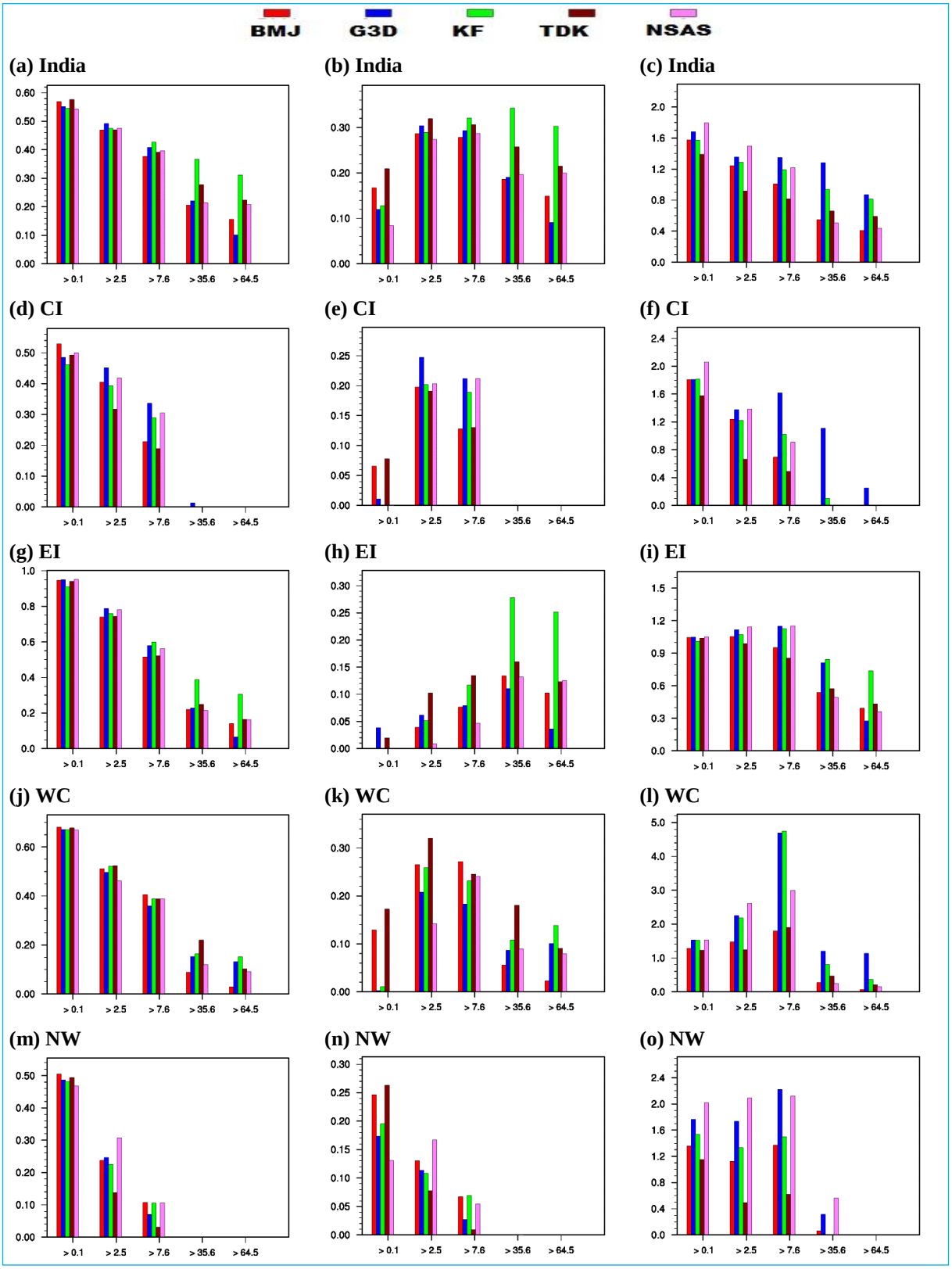

Figs. 9(a-o). Three categorical skill scores of day 2 forecasts for all physics experiments during case studies of 16-18 June, 2011. Left most panels for CSI, middle panels for GSS and right panels for BIAS scores. (a), (b) and (c) for all India, (d), (e) and (f) for CI, (g), (h) and (i) for EI, (j), (k) and (l) for WC and (m), (n) and (o) are for NW zones respectively

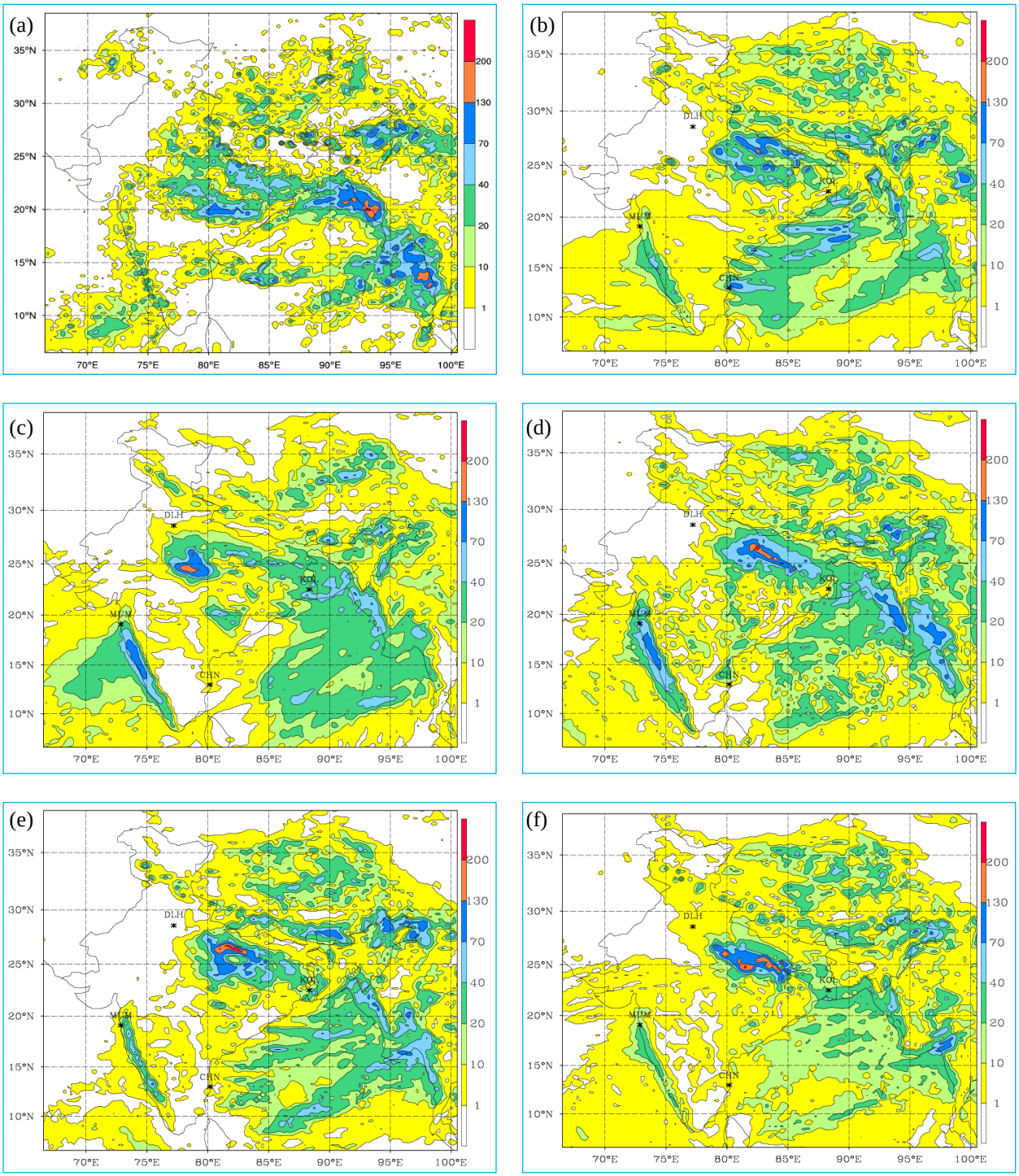

Figs. 10(a-f). Observed and day 1 forecasts of rainfall valid at 0300 UTC of 22nd July, 2011. (a) for observed TRMM rain and rainfall forecasts are for (b) BMJ, (c) G3D, (d) KF), (e) TDK and (f) NSAS respectively

reflected in the values of ETS and bias score for the specified zone. As the number of events at higher thresholds are very less, the miss number of the model is therefore is heightened and the scores must have lower values. The observed rainfall was distributed more over CI and NW zones and therefore, the scores over the zones in Case 2 show difference from case 1. The TDK has marked overestimation at 64.4 mm threshold over all zones except over WC and the same is reflected in all India value as well.

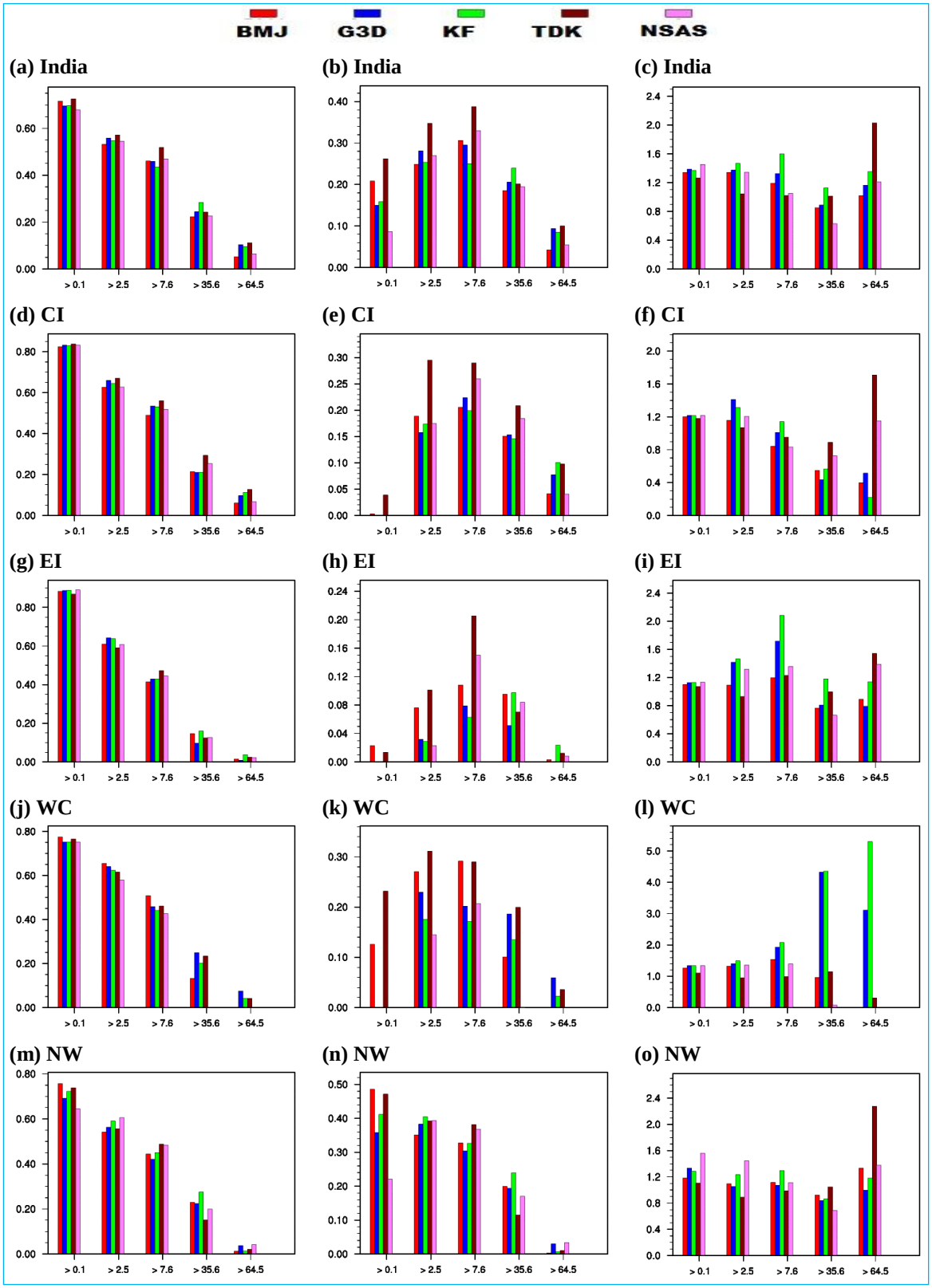

Figs. 11(a-o). Three categorical skill scores of day 1 forecasts for all physics experiments during case studies of 20-23 July, 2011. Left most panels for CSI, middle panels for GSS and right panels for BIAS scores. (a), (b) and (c) for all India, (d), (e) and (f) for CI, (g), (h) and (i) for EI, (j), (k) and (l) for WC and (m), (n) and (o) are for NW zones respectively

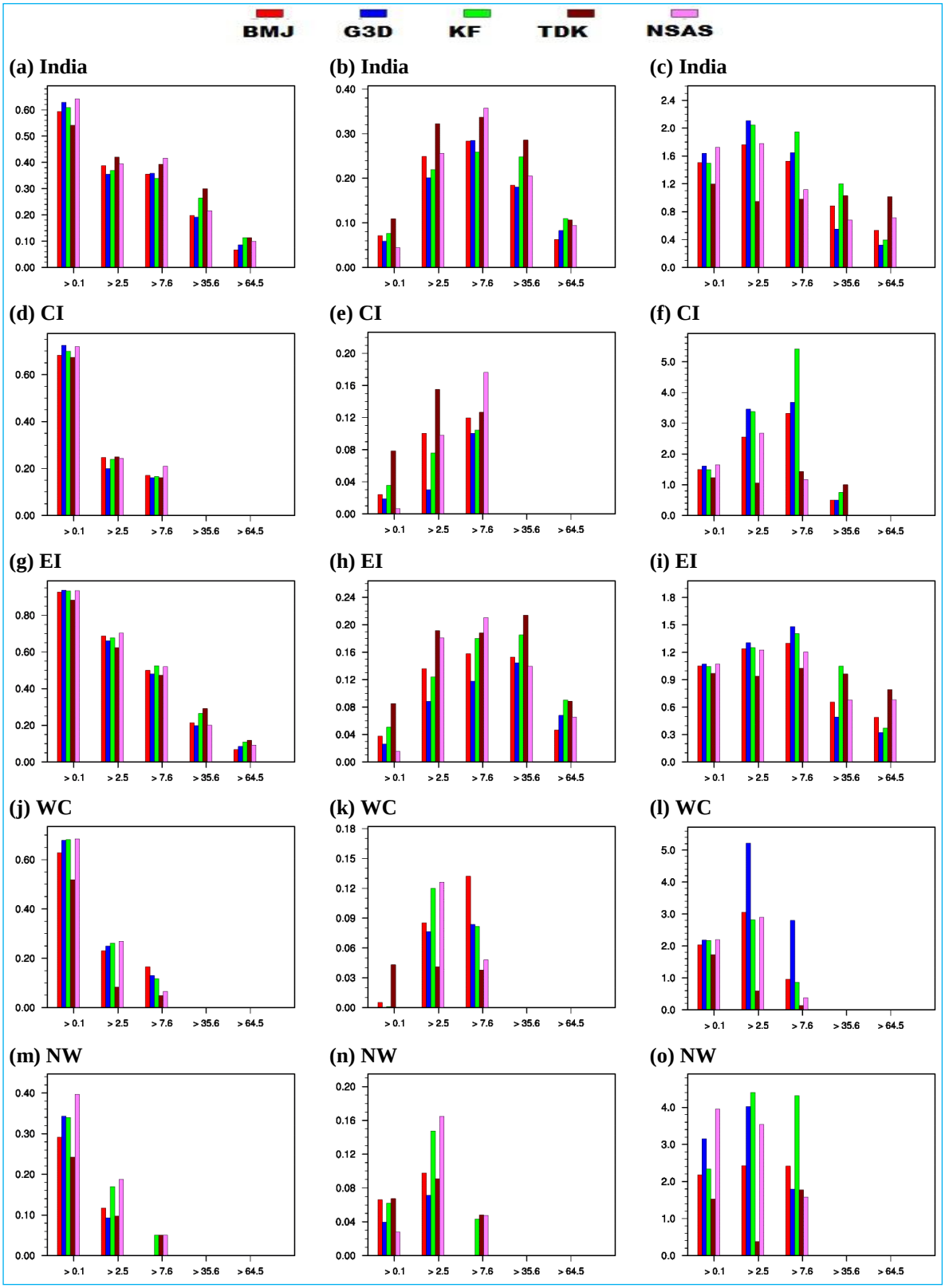

Figs. 12(a-o). Three categorical skill scores of day 1 forecasts for all physics experiments during case studies of 20-23 September, 2011. Left most panels for CSI, middle panels for GSS and right panels for BIAS scores. (a), (b) and (c) for all India, (d), (e) and (f) for CI, (g), (h) and (i) for EI, (j), (k) and (l) for WC and (m), (n) and (o) are for NW zones respectively

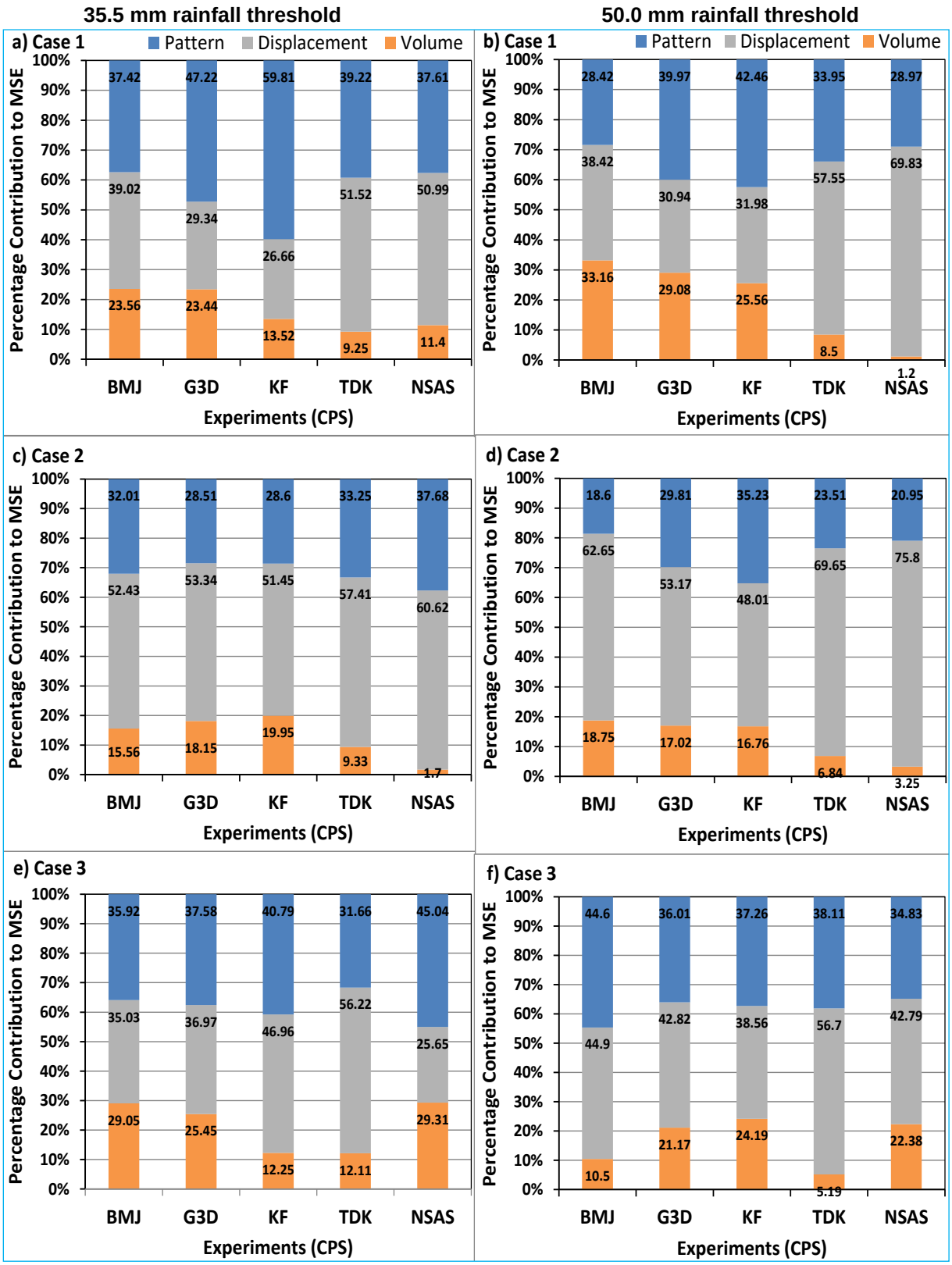

Figs. 13(a-f). CRA verification of day 1 forecasts of WRF model for all CPS experiments during three case studies. Partitioning of MSE in volume, displacement and pattern errors (a), (c) and (e) are for rain threshold of 35.5 mm and (b), (d) and (f) for rain threshold of 50.0 mm during case 1, case 2 and case 3 respectively

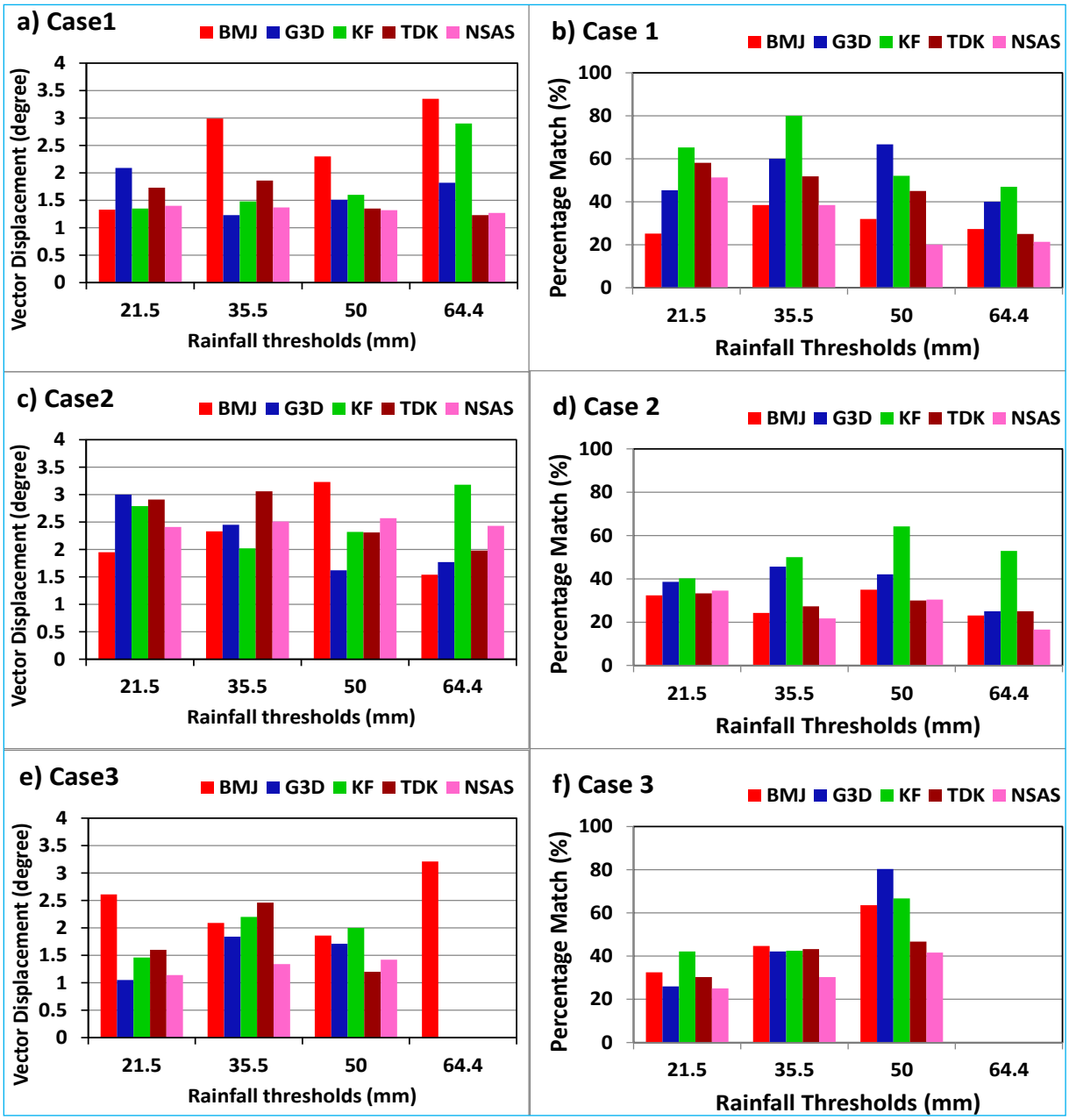

Figs. 14(a-f). CRA verification of day 1 forecasts of WRF model for all CPS experiments during three case studies. (a), (c) and (e) are vector displacements of rain objects and (b), (d) and (f) for percentages match during case 1, case 2 and case 3 respectively

Figs. 12(a-o) represent the average skill scores computed for 4 days during case 3 over Indian regions and other zones inside the same. All India values of the scores look similar to other two cases. The scores over EI somehow retain the familiar nature of the scores but other zones have significantly differences. The NW and CI regions received less rain during this period due to local convection and those events over these regions are poorly predicted by the model. The skill scores over these three zones (WC, NW and CI) demonstrate poor quality of the forecast irrespective of the CPS used in the model. Although, the WC has less rainfall, the GD has exceptionally large overestimation. In the same way, KF behaves over CI and over NW accompanied by NSAS.

Over all analysis of skill scores for all three cases, can bring out a little comparison between experiments. The TDK has consistent performance for all thresholds with an expected decline towards higher ranges. The overestimation of rainfall over G3D, KF and NSAS is

common up to moderate threshold. Still, the KF and G3D show better skills over the zones with rainfall due to orography and synoptic systems. Therefore, if we consider the performance of the model over all zones, no CPS amongst G3D, KF and TDK has any obvious advantage over others. The skill scores also depicted a few common characteristics of the model forecast over different zones at different thresholds. The skill scores show inadequate differences between the experiments during three separate events. The logical comparison between various CPSs is not practical in this manner.

3.2. *Verification of rainfall forecasts using CRA method*

The CRA method has diagnostic approach considering rain objects in the observed rainfall distribution and forecasts of the model as well. The method inspects the total error in terms of three partitions. Therefore, firstly the comparison amongst experiments will be done in terms of their error partitions during the three events. Figs. 13(a-f) demonstrate three partitions of errors for day 1 forecasts of all experiments considering only two thresholds just above moderate rainfall. The panels in the first row of the figure are for Case 1 weather event and other two rows represent the errors for other two cases sequentially.

The figure shows that the displacement has larger contribution in total MSE during Case 2 and 3 for two thresholds. For the calculation we considered the matched pairs of rain objects within observation and forecast. The percentage match for each forecast is computed to illustrate about the missed rain objects. Only observed rain objects have been searched within forecast. Contrary to that the forecast CRAs have not been searched in the observation in the present study. Therefore, a few rain objects falsely predicted have contribution in the total error and may be studied separately in future.

For larger amount of rain, the displacement clearly dominates over others. But, during Case 1, the model predicted the location the rain objects reasonably well and within total error, pattern has equal weightage with displacement. A few CPSs, e.g., G3D and KF have lower displacement error compared to others. During Case 2, all experiments indicate maximum displacement and least volume error. The overview of Figs. 10(a-f) also tells that the prominent observed rain areas due to depression has not been portrayed at proper location in the forecasts and therefore the probable matches have larger shifts. The quantitative measure of displacement in terms of vector shifting of the rain objects, the average values of the same for all experiments have been plotted in the bar diagrams of Figs. 14(a,c&e). The Fig. 14(c) shows the experiments have larger vector displacements during Case 2 episode compared to other two cases. The TDK and NSAS have smaller volume errors in Case 1 and 2 but KF in Case 3. But both experiments have less number of matched pair as shown in Figs. 14(b,d&f). In terms of percentage match for all three cases BMJ has lower values as it produced comparatively widespread rainfall amongst all CPSs and poorly captured observed rain objects. Although, G3D and TDK have comparable values of percentage match but KF has higher values considering every threshold during all three weather episodes. In terms of displacement KF has moderate shifting of CRAs. Although, NSAS have minute advantage in locating the rain areas at their right location but the capability of capturing observed rain areas with optimal similarity (based on CRA match criteria) is poorer than others. The group of G3D and KF earned superiority over others in the CRA verification whereas other group BMJ and NSAS showed reduced skill in predicting rain areas. The TDK falls in between these two groups of CPSs. The comparison of CPSs using diagnostic variables is followed in the next sub-section for further insight.

4. Summary and concluding remarks

The comparative verification of five different CPSs has been carried out using two separate methodologies. In the first approach, the standard categorical skill scores have been examined during weather episodes of 2011 associated with three different monsoon depressions. Secondly, CRA method has been employed to indicate the skill differential skills of 5 CPSs. Finally, diagnostic analysis in three ways has been completed for the very purpose of comparative evaluation of all CPSs. Many facts have been outlined and inferred from the investigations described above. A few points have been summarized based on the findings from three weather episodes and stated as follows :

(*i*) The skill scores have provided an overview about model performance for all CPSs. But, the obvious comparison between them could not be achieved. The poor performance by BMJ has been clearly notified exceeding moderate rain category. It has been found that all CPSs portrayed overestimation at all categories below heavy rain. There are three consistent performers with similar scores, *i.e*., G3D, KF and TDK. The KF and G3D have slight edge over others over the zones with elevated topography and synoptic systems.

(*ii*) The CRA method clearly shown the common forecast error characteristics in terms of displacement, volume and pattern errors. Although, all CPSs differed with varied error contributions from three parts, the displacement has the lions share. The volume error has the least significance and pattern has medium weightage for

MD forecast. From the computed percentage match along with vector displacements, the G3D and KF have small advantage over others.

The study targeted the comparison of CPSs in forecasting monsoon systems but the superiority of any scheme has not been established. As the rainfall is the diagnostic output of the model and mostly depends on convective parametrization, the study has given focus only on rainfall verification. The study brought out the fact that the model shows high variability in its skill with a change from one weather system to other, from one threshold to other and from one CPS to another. Following this uncertainty, it is inferred that a real-time configuration of a mesoscale model with a specific CPS is not capable enough to provide uniform and quality forecasts throughout the monsoon season for all weather events. Fritsch and Carbone (2004) has stated about the minute increases in quantitative precipitation forecast skill in utilizing several improvements in CPS of the model. The perfect precipitation forecast not only requires improved CPS but also other complex interactions amongst different physics (e.g., radiation, boundary layer, land-surface, soil model and explicit microphysical processes) in the model. Moreover, the uncertainty in the deterministic forecast may be addressed with ensemble approach using several member forecasts.

Acknowledgement

Authors are grateful to the Director General of Meteorology, India Meteorological Department for providing all facilities to carry out this research work. The NCAR, USA is also been acknowledged for the support and sharing of the community code of WRF modeling system. Earnest recognitions also go to CISL and DTC within NCAR for the NCAR Command Language (NCL) graphics software and Model Evaluation Tool (MET) which have been extensively used in the present study. Especially, authors are sincerely grateful to the anonymous reviewer for his valuable comments and suggestion to improvement of the research paper.

The contents and views expressed in this research paper are the views of the authors and do not necessarily reflect the views of their organizations.

References

Ardie, W. A., Sow, K. S., Tangang, F. T., Hussain, A. G., Mahmud, M. and Juneng, L., 2012, "The performance of different parameterization schemes in simulating the 2006/2007 southern peninsular Malaysia heavy rainfall episodes", *J. Earth Syst. Sci.*, **121**, 317-327.

Bosart, L. F., 2003, "Whither the weather analysis and forecasting process ?", *Wea. Forecasting*, **18,** 520-529.

Das, A. K., Bhowmick, M., Kundu, P. K. and Roy Bhowmik, S. K., 2015, "Verification of WRF Forecasts with TRMM Rainfall over India during Monsoon 2010 CRA Method", *Mausam*, **66**, 3, 403-414.

Das, A. K., Bhowmick, M., Kundu, P. K. and Roy Bhowmik, S. K., 2014, "Verification of WRF rainfall forecasts over India during monsoon 2010: CRA method", *Geofizika*, **31**, 105-126, doi: 10.15233/gfz.2014.31.6.

Deb, S. K., Srivastava, T. P. and Kishtawal, C. M., 2008, "The WRF model performance for the simulation of heavy precipitating events over Ahmedabad during August 2006", *J. Earth Sys. Sci.*, **117**, 589-602.

Ebert, E. E., William, A. and Gallus Jr., 2009, "Toward Better Understanding of the Contiguous Rain Area (CRA) Method for Spatial Forecast Verification", *Wea. Forecasting*, **24**, 1401-1415.

Fritsch, J. M. and Crabone, R. E., 2004, "Improving quantitative precipitation forecasts in the warm season: A USWRP research and development strategy", *Bull. Amer. Meteor. Soc.*, **85**, 955-965.

Grell, G. A. and Devenyi, D., 2002, "A generalized approach to parameterizing convection combining ensemble and data assimilation techniques", *Geophys. Res. Lett*., **29**, 14, 38-1-38-4.

Grell, G. A., 1993, "Prognostic Evaluation of Assumptions Used by Cumulus Parameterizations", *Mon. Wea. Rev*., **121**, 764-787.

Han, Jongil and Hua Lu, Pan, 2011, "Revision of convection and vertical diffusion schemes in the NCEP Global Forecast System", *Wea. Forecasting*, **26**, 520-533.

Houze, R. A. Jr., 1997, "Stratiform precipitation in regions of convection: a meteorological paradox?", *Bull. Amer. Meteor. Soc.*, **78**, 2179-2196.

Janjic, Zavisa I., 1994, "The Step-Mountain Eta Coordinate Model: Further developments of the convection, viscous sublayer and turbulence closure schemes", *Mon. Wea. Rev*., **122**, 927-945.

Kain, John S., 2004, "The Kain-Fritsch convective parameterization: An update", *J. Appl. Meteor*., **43**, 170-181.

Kanase, R. D. and Salvekar, P. S., 2014, "Study of Weak Intensity Cyclones over Bay of Bengal Using WRF Model", *Atmospheric and Climate Sciences*, **4**, 534-548, doi:10.4236/acs.2014.44049.

Kolusu, S. R., Venkatraman, Prasanna and Preethi, B., 2013, "Simulation of Indian summer monsoon intra-seasonal oscillations using WRF regional atmospheric model", *Int. J. Earth Atmos. Sci*., **1**, 35-53.

Lim, K. S. S., Hong, S. Y., Yoon, J. H. and Han, J., 2014, "Simulation of the Summer Monsoon Rainfall over East Asia Using the NCEP GFS Cumulus Parameterization at Different Horizontal Resolutions", *Wea. Forecasting*, **29**, 1143-1154.

Mapes, B. E., 1977, "Equilibrium vs. activation control of large-scale variation of tropical deep convection", *The Physics and Parameterization of Moist Atmospheric Convection*, Ed. R. K. Smith, Kluwer Academic Publishers, 321-358.

Mukhopadhyay, P., Taraphdar, S., Goswami, B. N. and Krishna Kumar, K., 2010, "Indian summer monsoon precipitation climatology in a high resolution regional climate model: Impact of convective parameterization on systematic biases", *Weather and Forecasting*, **25**, 369-387, doi: 10.1175/2009WAF2222320.1.

Osuri, K. K., Mohanty, U. C., Routray, A., Kulkarni, M. A. and Mohapatra, M., 2012, "Customization of WRF-ARW Model with Physical Parameterization Schemes for the Simulation of

Tropical Cyclones over North Indian Ocean", *Natural Hazards*, **63**, 1337-1359, http://dx.doi.org/10.1007/s11069-011-9862-0.

Raju, A., Parekh, A. and Gnanseelan, C., 2013, "Evolution of vertical moist thermodynamic structure associated with the Indian summer monsoon 2010 in a regional climate model", *Pure Applied Geophysics*, **171**, 7, 1499-1518, doi:10.1007/s00024-013-0697-3.

Randall, D. A., Abeles, J. A. and Corsetti, T. G., 1985, "Seasonal simulations of the planetary boundary layer and boundary-layer stratocumulous clouds with a general circulation model", *J. Atmos Sci.*, **42**, 641-675.

Skamarock, W. C. and Weisman, M. L., 2009, "The Impact of Positive-Definite Moisture Transport on NWP Precipitation Forecasts", *Mon. Wea. Rev*., **137**, 488-494, doi:http://dx.doi.org/10.1175/2008MWR2583.1

Skamarock, W. C., Klemp, J. B., Dudhia, J., Gill, O., Barker, D. M., Wang, W. and Powers, J. G., 2005, "A description of the Advanced Research WRF Version 2", NCAR Technical Note, NCAR/TN-468+STR, p100, doi:10.5065/D6DZ069T.

Taraphdar, S., Mukhopadhyay, P. and Goswami, B. N., 2010, "Predictability of Indian summer monsoon weather during active and break phases using a high resolution regional model", *Geophysical Research Letters*, **37**, L21812, 1-6, doi:10.1029/2010GL044969.

Tiedtke, M., 1989, "A comprehensive mass flux scheme for cumulus parameterization in large-scale models", *Mon. Wea. Rev.*, **117,** 1779-1800.

Tribbia, J. J., 1991, "The rudimentary theory of atmospheric teleconnections associated with ENSO", *Teleconnections Linking Worldwide Climate Anomalies*, ed. M. H. Glantz, R. W. Katz and N. Nicholls, Cambridge University Press, 285-308.

Wang, Y. C. and Tung, W. W., 2010, "Impacts of cloud-system resolving regional modeling on the simulation of monsoon depressions", *Geophys. Res. Letters.*, **37**, L08806, doi:10.1029/2010 GL042734.

Yu, E., Wang, H., Gao, Y. and Sun, J., 2011, "Impacts of cumulus convective parameterization on summer monsoon precipitation over China", *Acta Meteorol. Sinica*, **25**, 581-590.

Zhang, Chunxi, Wang, Yuqing and Hamilton, Kevin, 2011, "Improved representation of boundary layer clouds over the southeast pacific in ARW-WRF using a modified Tiedtke cumulus parameterization scheme", *Mon. Wea. Rev.*, **139**, 3489-3513.